Residual static corrections by means of CRS attributes

I. Koglin and E. Ewig

email: *Ingo.Koglin@gpi.uni-karlsruhe.de*
keywords: *residual, static, correction, CRS, moveout*

ABSTRACT

Residual static corrections are of great interest for onshore datasets. There, they are used to eliminate the influence on reflection traveltimes of mostly the weathering layer or the errors of redatuming methods. Thus, the results of stacking methods applied after residual static corrections should show an improved signal-to-noise (S/N) ratio. We considered to make use of the common-reflection-surface (CRS) stack which gives additional information about the subsurface by the CRS attributes. Here, the CRS attributes serve as a basis for the moveout correction which is important for determining the residual statics. The theoretical background introduces to the residual static correction problem and the first results of a synthetic test show that our new approach is able to estimate residual statics adequately.

INTRODUCTION

Onshore real data acquisition is often influenced by topography and irregularities in the near-surface, i. e., the weathering layer. The topographic effect on the reflection times is significantly removed by applying so-called field static corrections. However, the rapid changes in elevation and in near-surface velocity or thickness of the weathering layer still remain as reflection time distortions. To eliminate these remains which the field static correction did not compensate, the residual static correction assigns every shot and every receiver an additional static time shift. The time shifts of residual static corrections aim to enhance the continuity of reflection events and to improve the signal-to-noise (S/N) ratio after stacking.

The 2D zero-offset (ZO) common-reflection-surface (CRS) stack method has shown its abilities to improve the S/N ratio even for noisy data assuming a horizontal plane measurement surface (see Trappe et al., 2001). Zhang and Hubral (2002) have introduced the topography into the CRS stack method which can be seen as a kind of field static correction. But so far, the 2D ZO CRS stack method does not yet account for residual static corrections. Thus, a new approach of residual static correction based on the CRS attributes is presented in the following.

BASICS OF STATIC CORRECTIONS

The main assumption for applying "static" corrections is the surface consistency. This means that the rays propagate nearly vertical through the uppermost layer and, hence, independent from the raypaths in the deeper layers. Thus, the time shifts become properties of the source or receiver locations, respectively. Furthermore, the reflection time distortions do not depend on the traveltime of different reflection events, i. e., are reflection time independent and, therefore, these time shifts are called "static" corrections. Another assumption is that the uppermost layer, i. e., the weathering layer, has the same influence on the shape of the wavelet of all emerging reflection events.
Under these assumptions, static corrections are divided into two parts:

- The field static correction which is a kind of redatuming introduces a "datum plane" as substitute beneath the weathering layer (see Figure 1). For further explanation, please refer to Marsden (1993).

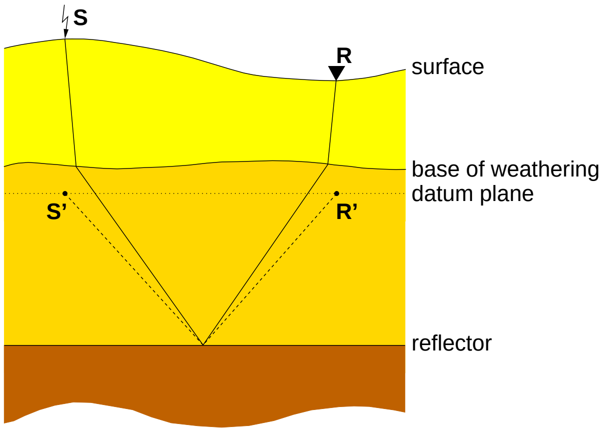

Figure 1: Raypath with a low velocity layer. Redatuming achieved by field static correction substitutes the surface by a datum plane beneath the low velocity layer, i. e., source S and receiver R are moved to S' and R' on the datum plane, respectively.

- The residual static correction is used to eliminate small variations of reflection traveltimes caused by the weathering layer. Additionally, errors from redatuming by field static correction or other methods can be removed. Even though, residual static corrections can be also applied without other preceeding static corrections to enhance the imaging quality.

Conventional residual static correction methods

To achieve surface consistency, residual static correction techniques have to provide one exclusive time shift for every source or receiver corresponding to one common-shot (CS) or common-receiver (CR) gather, respectively. The first step of most conventional residual static correction techniques is to apply an approximate NMO correction. Then, the reflection events in each gather are considered to be misaligned due to a source static, a receiver static, and residual moveout. The calculated time shifts t_{ij} of every trace are related according to

$$t_{ij} = r_i + s_j + G_k + M_k X_{ij}^2 \quad \text{with} \quad k = \frac{i+j}{2} \tag{1}$$

where r_i is the receiver static of the i-th receiver location and s_j is the source static for the j-th source location. G_k, the structural term, is an arbitrary time shift for the k-th CMP gather and depends on the subsurface structure, M_k is the residual moveout at the k-th CMP gather, and $X_{ij} = s_j - r_i$ is the source to receiver distance (see Taner et al., 1974; Wiggins et al., 1976; Cox, 1974). Figure 2 shows an example of the improvements of residual static corrections for the stacking result. Figure 2(a) shows a reflection event after NMO correction distorted by residual statics. Stacking these traces without any corrections results in dislocated peaks for this reflection event and also a deformed wavelet (see Figure 2(b)), while the stack with residual static correction clearly shows an undeformed wavelet with larger amplitudes due to the coherent stack (see Figure 2(c)).

One technique to obtain t_{ij} is to cross correlate all traces of each CMP gather with its corresponding CMP stacked trace as pilot trace. The window for correlation has to be selected to cover more than one dominant primary event (time invariance) and at reasonably large traveltimes (surface consistency). Thus, a system of simultaneous equations of t_{ij} is given by one equation for each trace of the whole dataset. This large system of linear equations is overdetermined, i. e., there are more equations than unknowns, and underconstrained, i. e., there are more unknowns than independent equations. The solution is generally obtained by least-square techniques.

Ronen and Claerbout (1985) introduced a stack power maximization technique based on cross correlation. Here, the cross correlation is performed between so-called "super-traces". A super-trace built from all the traces of the shot profile in sequence (trace F in Figure 3) is cross correlated with another super-trace

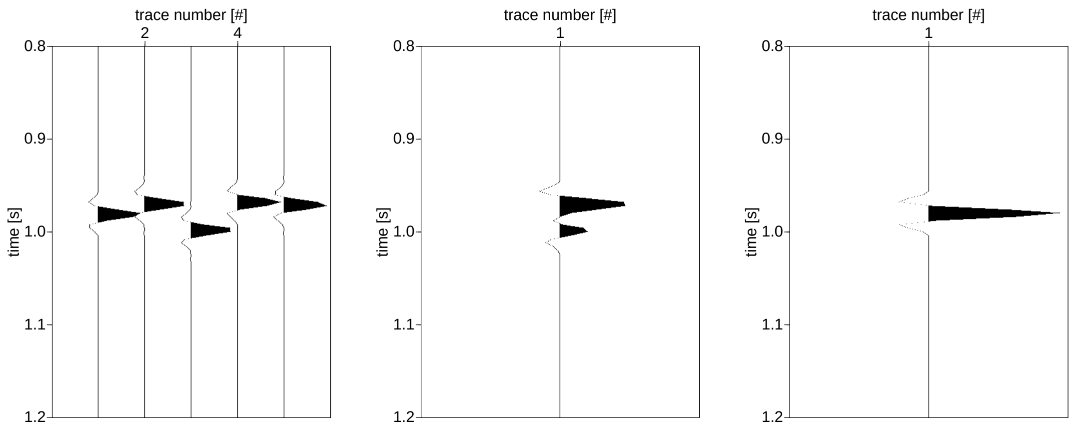

(a) synthetic gather **(b)** stacked 'as is' **(c)** with residual static correction

Figure 2: Example of residual static correction enhancement after an approximate NMO correction was applied.

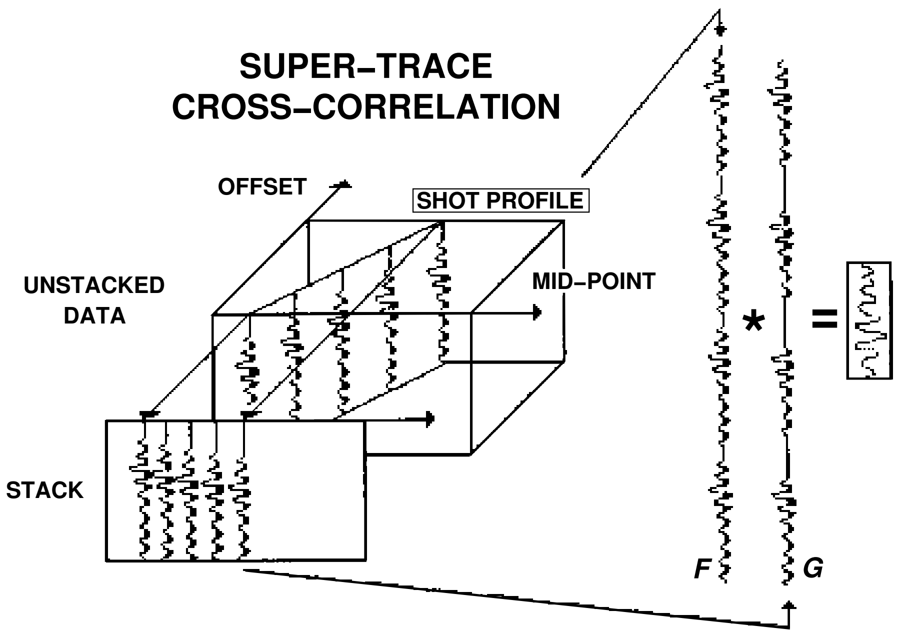

Figure 3: Example of super-traces for one moveout corrected shot gather. Super-trace F and super-trace G are cross correlated to determine the corresponding source static. Figure taken from Ronen and Claerbout (1985).

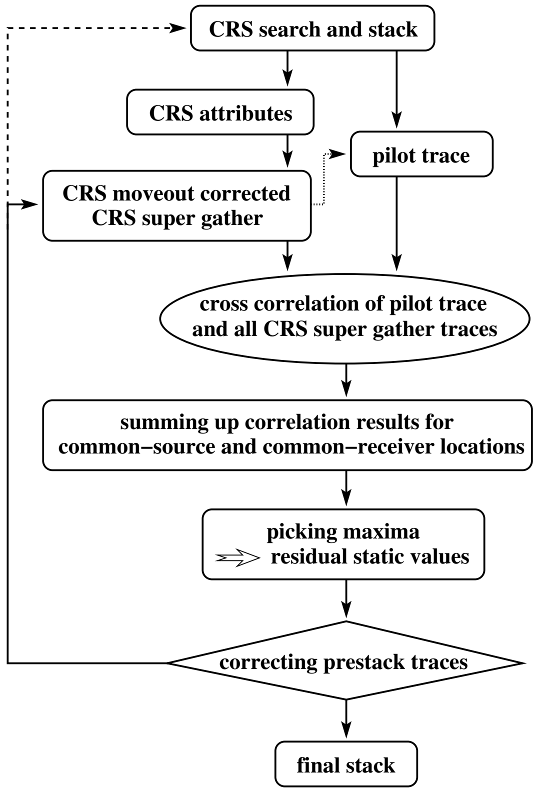

Figure 4: Flowchart for the iterative residual static correction by means of CRS attributes. For the second and further iterations, the CRS search for the attributes can be optionally performed again but this will need more processing time. If not, the pilot trace has to be recalculated from the CRS moveout corrected CRS super gather to take advantage of the enhancements of the first or previous iterations.

built of all traces in the relevant part of the stack in sequence without the contribution of that shot (trace G in Figure 3). The source static of this shot is the picked maximum of the cross correlation. This procedure is repeated for every shot and receiver profile, respectively. The resulting time shifts maximize the sum of squares of the final stack, i. e., the stack power.

NEW APPROACH BY MEANS OF CRS ATTRIBUTES

The CRS stack method provides additional sections, one for each CRS attribute. These attributes (α, R_{NIP}, R_{N}) are parameters of the stacking surface given by

$$t^2_{hyp}(x,h) = \left[t_0 + \frac{2}{v_0}(x-x_0)\sin\alpha\right]^2 + \frac{2}{v_0}t_0\cos^2\alpha\left[\frac{(x-x_0)^2}{R_{\mathrm{N}}} + \frac{h^2}{R_{\mathrm{NIP}}}\right], \tag{2}$$

with the ZO traveltime t_0, the near-surface velocity v_0, the emergence angle α of the ZO ray, the radius of curvature of the NIP wavefront R_{NIP} measured at x_0, and the radius of curvature of the normal wavefront R_{N} also measured at x_0. This stacking surface from the CRS stack method improves the S/N ratio even more than, e. g., the NMO/DMO/stack method (see Mann, 2002; Müller, 1999; Trappe et al., 2001).

Our new approach is based on cross correlations and is similar to the technique of Ronen and Claerbout (1985). Figure 4 shows the principal steps of our method. The very first step is to perform at least the initial 2D ZO CRS stack to obtain the CRS attribute sections and the simulated ZO section. Each trace of the simulated ZO section will serve as a pilot trace for the necessary cross correlations. Additionally, the optimized 2D ZO CRS stack can also be used for the following steps but this requires more processing time due to the optimization. Then, the CRS moveout correction is realized with the previously obtained CRS attributes.

CRS moveout correction

To correct for the CRS moveout, the half-offset h and midpoint x dependency of equation (2) has to be eliminated. Therefore, the CRS attributes of every time sample are required. These attributes are provided by the initial or optimized search of the CRS stack method. With the knowledge of these attributes, the common-reflection-surface can be transformed into a horizontal plane at time t_0 by subtracting the moveout given by

$$t_{moveout}(x,h) = t_{hyp}(x,h) - t_0, \tag{3}$$

where t_0 is given by the considered time sample of the simulated ZO section.

This correction is performed for all t_0 given by each simulated ZO trace of the CRS stack. The result for one ZO trace is called "CRS super gather" and contains all CRS moveout corrected prestack traces which lie inside the corresponding CRS aperture. Thus, the prestack traces are multiply contained in the CRS super gathers but with different moveout corrections.

Cross correlation

The difference to the super-trace cross correlation method of Ronen and Claerbout (1985) is that the cross correlations are not performed between the super-traces but as correlation of every single moveout corrected trace with the pilot trace. Afterwards, all correlation results that belong to the same source or receiver location are summed up. Finally, the residual static value is given by the time associated with the maximum of the summed correlation results. The correlation of the super-traces accounts for the subsurface structure because super-trace G of Figure 3 is a sequence of neighboring stacked traces and not of one stacked trace repeated multiple times. Super-trace F consists of all traces belonging to the same source or receiver location, respectively. The CRS stack accounts for the subsurface structure by means of the CRS attribute R_{N} which enters into the CRS moveout correction. R_{N} is the radius of curvature of the normal wave measured at the surface and can be associated with the hypothetical exploding reflector experiment.

Problems might occur at the boundary of the dataset because there only few correlation results will contribute to source or receiver locations. Therefore, we implemented a limit for the maximum correlation shift, i. e., a maximum residual static limit. In future, the picking the maximum of the summed cross correlations will also check the near neighborhood for local maxima to decide whether the global maxima is reliable or not.

Iteration

After the residual static values are obtained from the cross correlation results, the prestack traces are time shifted with the corresponding total time shifts. The total time shift is simply the sum of the corresponding source and receiver static values of each prestack trace. If the CRS stack of these corrected prestack traces is not yet satisfactory, the entire procedure can be started again in two different ways. One way is to perform the CRS search and all other steps as in the first iteration (see dashed line in Figure 4). The other way is to assume that the CRS attributes found in the first iteration are the "true" attributes and therefore the CRS search is omitted (illustrated by the dotted line in Figure 4). As the CRS search is time consuming, it is attractive to omit this step. But on the other hand, it might be dangerous to rely on the CRS attributes: if the time shifts between neighboring traces are too large, the CRS stack propably fails to detect actually contigious events and the corresponding attributes.

SYNTHETIC MODEL AND FIRST RESULTS

We started with a very simple isotropic model with four layers separated by three reflectors (see Figure 5). The first reflector was chosen to be a horizontal plane, the second a dipping plane, and the third one includes a syncline. The layer velocities are from top to bottom: $v_1 = 2.2$ km/s, $v_2 = 2.5$ km/s, $v_3 = 3.0$ km/s, and $v_4 = 3.5$ km/s. Figure 6 shows the result of the optimized 2D ZO CRS stack from the original model without statics and, in contrast, the result with random but surface consistent residual statics. We based our further calculations on the optimized CRS attributes as we have once calculated them to test the reliability of the initial CRS attributes. The optimization did not show significant changes in the attribute

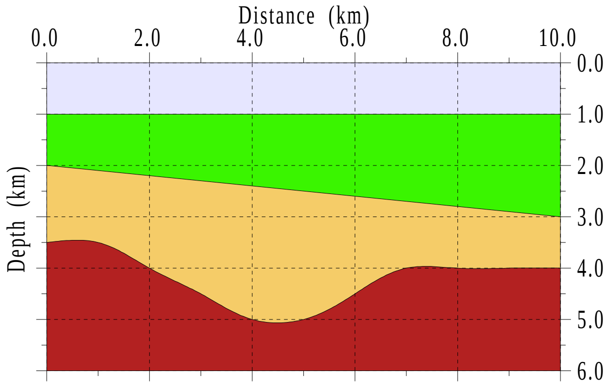

Figure 5: Synthetic 2D model with four constant velocity layers. $v_1 = 2.2$ km/s, $v_2 = 2.5$ km/s, $v_3 = 3.0$ km/s, and $v_4 = 3.5$ km/s from top to bottom.

sections or the simulated ZO section due to the simple model. Thus, also the results of the initial CRS stack can be used.

From the optimized CRS search, the CRS attributes served as input for the CRS moveout correction. Figure 7 shows only a part of one moveout corrected CRS super gather at CMP 120 because in our case a CRS super gather can contain up to 3499 traces. It is obvious that the CRS moveout correction has flattened the reflection events and that they are dislocated due to the randomly added residual source and receiver statics. Also the time invariance becomes clear if one compares the dislocation of the contained reflection events.

Now, we are able to perform the cross correlations of the first iteration. The CRS moveout corrected traces of CRS super gathers are correlated with their corresponding pilot traces which are the simulated ZO traces from the CRS stack. The results are summed up for common shot or receiver locations, respectively. Then, the next CRS super gather is processed. In general, this yields more than one correlation result for every shot or receiver from one CRS super gather. But also from neighboring CRS super gathers, correlation results will contribute to the total correlation sum as long as the shot or receiver is contained in the CRS aperture. Thus, picking the maximum of the summed cross correlation results after all CRS super gather are processed directly gives the separated source and receiver static values. Figures 8 show the added random residual static values as solid lines for some source and receiver locations. The dashed/dotted lines are the obtained residual static values after 10/40 CRS super gathers have contributed to the picking of global maxima from the cross correlation sums. In some cases, the obtained residual static values became worse but over all they improve the more CRS super gathers contribute. The total residual correction for each trace is the sum of the corresponding source and receiver static values.

The last step for the first iteration is to shift the prestack traces by the just obtained total residual static values. The improvements of the first iteration are illustrated in Figure 9. Figure 9(a) shows the original CMP gather at CMP 120, Figure 9(b) is the same CMP gather but with random residual statics, and Figure 9(c) displays the CMP gather after the residual static correction was performed with the results of the first iteration of our new approach. The residual static corrected CMP gather is close to the original one. There are still some residual statics remaining which will be eliminated by further iterations as the pilot traces will gain from the improved S/N ratio and the improved CRS attributes of the second CRS search.

CONCLUSIONS

Residual static corrections are, in general, based on cross correlations. We showed that the CRS stack method can help to derive the residual statics. Here, the advantages of the CRS stack method, i. e., the improved S/N ratio and the additional information about the subsurface by the CRS attributes compared to, e. g., the NMO/DMO/stack, is integrated into our new approach. The CRS attributes fit surfaces closer to reflection events which is essential for a good moveout correction, and the traces of the simulated ZO section are better pilot traces than simply CMP stacked traces. Our new approach combines the conventional methods (cross correlation, picking maxima) with the improvements of the CRS stack. Here, the large

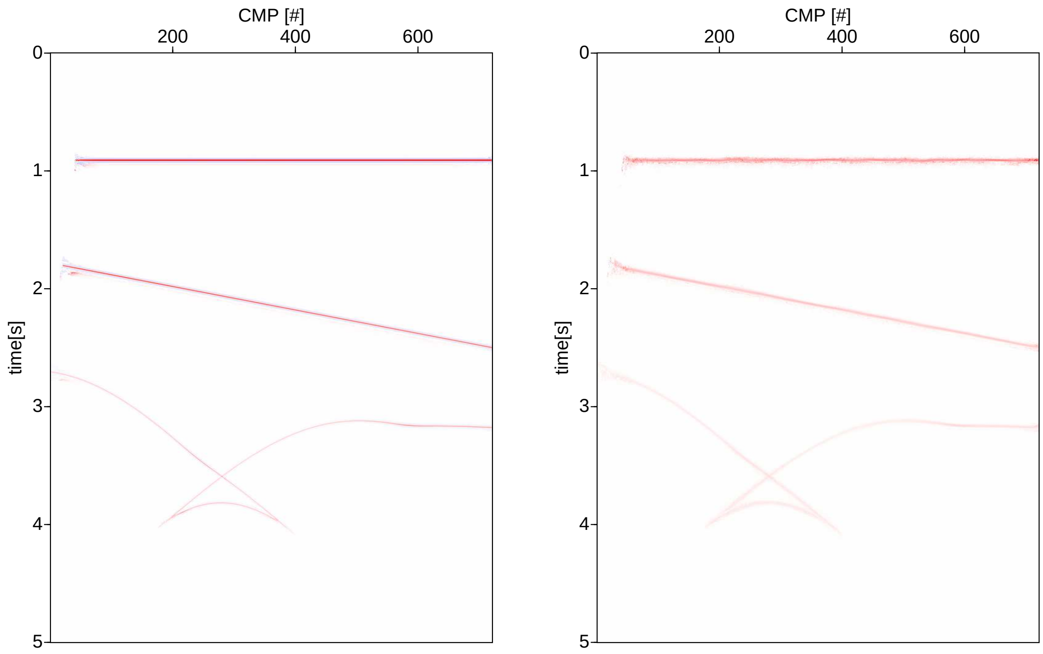

(a) original **(b)** with random residual statics

Figure 6: Simulated ZO section of the optimized 2D ZO CRS stack from a) the original synthetic data set and b) with random residual statics added.

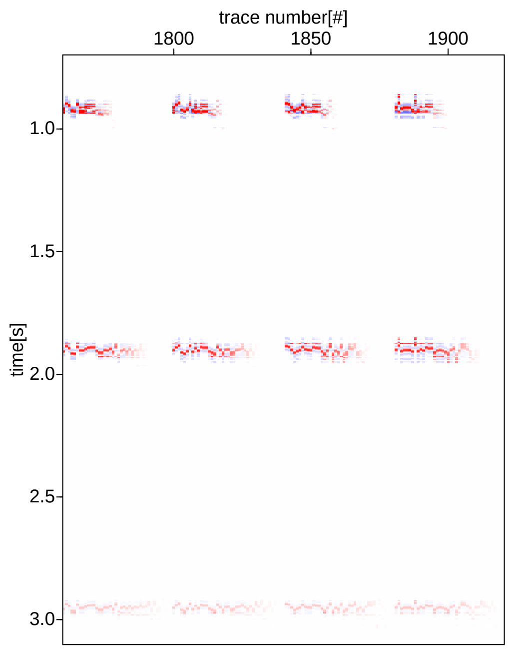

Figure 7: This is a part of the CRS moveout corrected CRS super gather for CMP 120. The CMPs within the CRS aperture are shown one after the other and their traces are consecutively numbered. It is obvious that the moveout correction did not correct the random residual statics. The reflection events are more or less flattened.

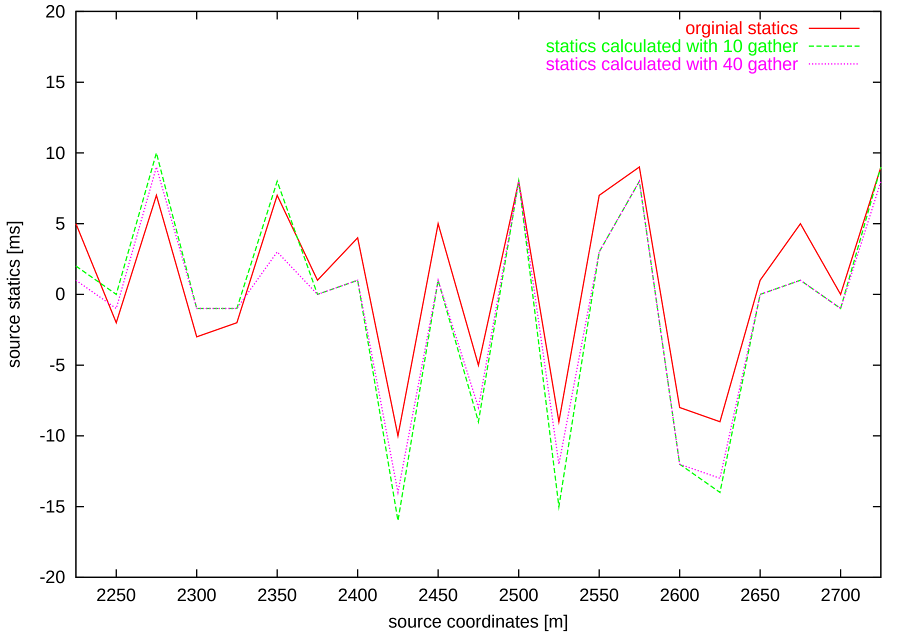

(a) obtained source residual statics

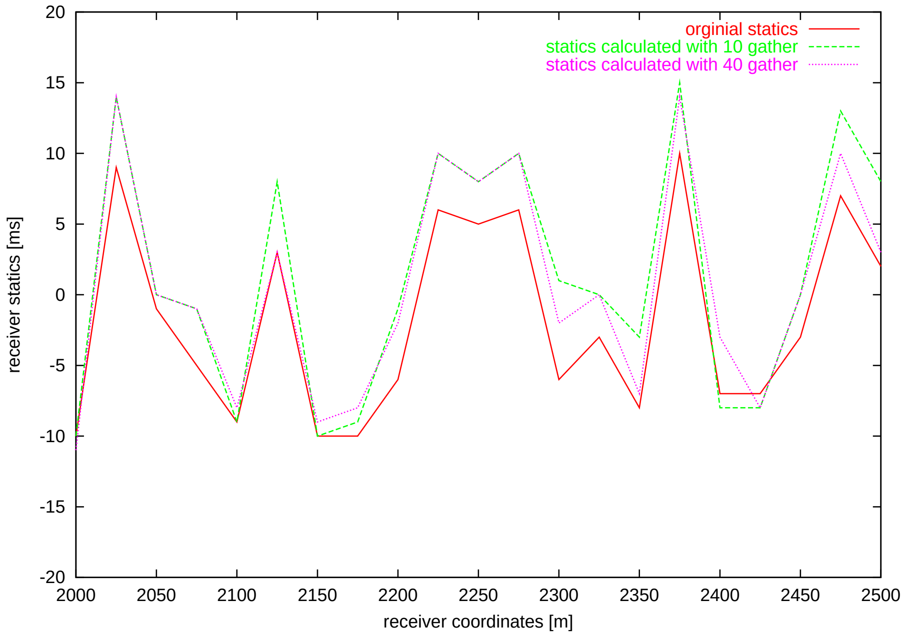

(b) obtained receiver residual statics

Figure 8: Residual static values. Added random statics are displayed as solid lines. The dashed lines are the picked residual statics after 10 CRS super gathers have contributed to the correlation sum and the dotted lines after 40 CRS super gathers have contributed.

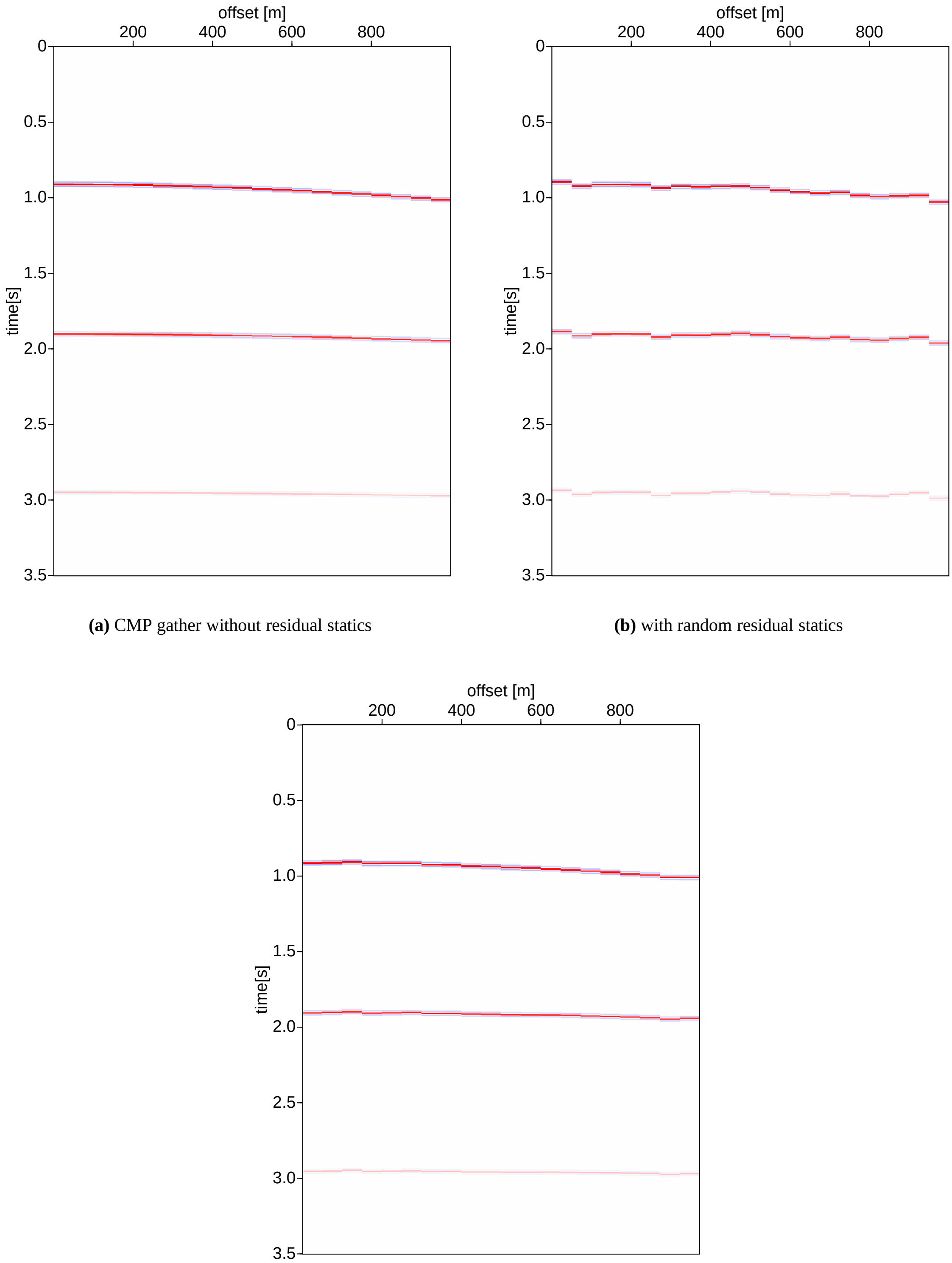

(a) CMP gather without residual statics

(b) with random residual statics

(c) with residual static correction

Figure 9: Example of residual static correction enhancement after the first iteration of our new approach displayed at CMP 120.

spatial aperture of the CRS stack takes more traces into account than just correlating within CMP gathers.

As displayed in Figure 9, the results of the first synthetic test showed that this new approach is able to enhance the simulated ZO section of datasets distorted by residual statics. Thus, more effort will be put in the determination of the residual static values in the future. Despite of simply picking the global maximum of the summed cross correlation results, also the neighboring maxima can be accounted for to evaluate the reliability of the results.

ACKNOWLEDGEMENTS

This work was kindly supported by the sponsors of the *Wave Inversion Technology (WIT) Consortium*, Karlsruhe, Germany. We also thank Dr. Franz Kirchheimer for his ideas and suggestions.

REFERENCES

Cox, M. (1974). *Static Correction for Seismic Reflection Surveys*. Society of Exploration Geophysicists.

Mann, J. (2002). *Extensions and Applications of the Common-Reflection-Surface Stack Method*. Logos Verlag, Berlin.

Marsden, D. (1993). Static corrections—a review. *The Leading Edge*, 12(1):43 – 49.

Müller, T. (1999). *The Common Reflection Surface Stack Method - Seismic imaging without explicit knowledge of the velocity model*. Der Andere Verlag, Bad Iburg.

Ronen, J. and Claerbout, J. F. (1985). Surface-consistent residual statics estimation by stack-power maximization. *Geophysics*, 50(12):2759 – 2767.

Taner, M. T., Koehler, F., and Alhilali, K. A. (1974). Estimation and correction of near-surface anomalies. *Geophysics*, 39(4):441 – 463.

Trappe, H., Gierse, G., and Pruessmann, J. (2001). Case studies show potential of Common Reflection Surface stack – structural resolution in the time domain beyond the conventional NMO/DMO stack. *First Break*, 19(11):625 – 633.

Wiggins, R. A., Larner, K. L., and Wisecup, R. D. (1976). Residual static analysis as a general linear inverse problem. *Geophysics*, 41(5):922 – 938.

Zhang, Y. and Hubral, P. (2002). 2D ZO CRS stack and redatuming for a complex top surface topography. In *Extended Abstracts*, pages 2051 – 2053, Session SP 1.6. 72nd Annual Internat. Mtg., Soc. Expl. Geophys.